

OFDM Pilot Design for Channel Estimation with Null Edge Subcarriers

Benjamin R. Hamilton, Xiaoli Ma, John E. Kleider, and Robert J. Baxley

Abstract—Wireless communication systems are increasingly adopting orthogonal frequency division multiplexing (OFDM) to enable efficient high-data rate transmissions. Such systems often employ pilot symbols to estimate wireless channels, and null subcarriers on band edges to reduce adjacent channel interference. Recent work has focused on designing the pilot sequence to improve channel estimation performance. In this paper, we present a new pilot design for OFDM systems based on a arbitrary-order polynomial parameterization of the pilot subcarrier indices. We show our design achieves better performance than existing methods. Theoretical models and simulated performance demonstrate the increased accuracy of our design.

Index Terms—OFDM, pilot design, channel estimation.

I. INTRODUCTION

ORTHOGONAL frequency division multiplexing (OFDM) has become an increasingly common technique in communication systems and has been adopted by many standards (e.g. IEEE 802.16 [1]). An important advantage of OFDM is that it allows for simple and robust compensation of the effects of multipath channels [2]. Since this robustness directly relies on having accurate estimates of the wireless channel, pilot symbol assisted modulation (PSAM) [3], where known pilot tones are inserted into OFDM symbols, has been proposed to allow for low complexity channel estimation. Previous works [4]–[8] have shown that optimizing the pilot position and power can significantly improve channel estimator performance. It has been shown that for OFDM systems where all of the subcarriers are in use, the pilot design which minimizes the mean squared error (MSE) consists of equally spaced pilots of uniform power [9]–[11]. In practice, however, not all of the subcarriers in an OFDM system are available for information transmission. Some of the subcarriers on the band edges are designated “null subcarriers,” which must not be occupied. While the null subcarriers reduce interference between adjacent bands, they complicate pilot design. The frequency response of the channel can be seen as a band-limited periodic signal.

Manuscript received October 28, 2010; revised March 11, 2011 and June 13, 2011; accepted August 13, 2011. The associate editor coordinating the review of this letter and approving it for publication was D. Michelson.

B. R. Hamilton and X. Ma are with the School of Electrical and Computer Engineering, Georgia Institute of Technology, Atlanta, GA 30332 (e-mail: bhamilton3@mail.gatech.edu, xiaoli@ece.gatech.edu).

J. Kleider is with General Dynamics C4 Systems, Atlanta, GA 30308 (e-mail: John.Kleider@gdc4s.com).

R. Baxley is with the Georgia Tech Research Institute, Atlanta, GA 30332 (e-mail: Bob.Baxley@gtri.gatech.edu).

Prepared through collaborative participation in the Communications and Networks Consortium sponsored by the U. S. Army Research Laboratory under the Collaborative Technology Alliance Program, Cooperative Agreement DAAD19-01-2-0011. The U. S. Government is authorized to reproduce and distribute reprints for Government purposes notwithstanding any copyright notation thereon.

Digital Object Identifier 10.1109/TWC.2011.090611.101922

Without null subcarriers, we can space the pilots uniformly and effectively sample the frequency response at the Nyquist rate. Adding null subcarriers has two effects on the pilot design: 1) we can no longer place the pilots at the Nyquist interval so we must perform nonuniform sampling and 2) we no longer need to estimate the channel frequency response for the null subcarriers.

Several design techniques for systems with null subcarriers have been proposed. Song et al. [12] extended the equally spaced pilot design to systems with null subcarriers using partially equispaced subcarriers, which was extended to MIMO OFDM in [13]. In [4], [5], the pilot position was parameterized using a cubic polynomial and a grid search of the parameter space was used to obtain an approximation of the optimal pilot placement. An iterative reduction method [6]–[8] was proposed, where a pilot design with more than the desired number of pilots is iteratively reduced to a design with the desired number of pilots by discarding pilot tones that are assigned the lowest power. Both the pilot parameterization and the iterative reduction techniques use convex optimization to determine the power profile numerically. While these techniques are effective in systems where the channel is relatively short and the number of pilots is small, we have found these designs are increasingly suboptimal in systems with more pilots and longer channels.

In this paper, we derive an analytical solution for the pilot power profile which minimizes the MSE of the least-squares channel estimate for an arbitrary pilot placement. We also demonstrate the 3rd order parameterization of [4] produces a design with a relatively high MSE for systems with longer channels and larger numbers of subcarriers. We propose a framework for higher order parameterizations for pilot design in such systems and derive the bounds for the grid search over the parameterization variables. We use numerical examples to show that the design produced using a 5th order parameterization has a lower theoretical MSE than those from the 3rd order parameterization [4], the partially equispaced subcarriers design [12], and the iterative reduction method [8]. We verify this theoretical MSE against the MSE and bit-error rate (BER) estimates through Monte Carlo simulation.

II. SYSTEM MODEL

Consider an OFDM system with a total N subcarriers. Of these, N_p subcarriers are used as pilots for channel estimation, and N_{null} are null subcarriers on the band edges. The remaining N_d subcarriers are available for data transmission.

The OFDM modulated data signal x is transmitted through an L_h -tap channel, h , and received as y . This is represented in the time domain as

$$y[n] = \sum_{l=0}^{L_h-1} h[l]x[n-l] + w[n], \quad (1)$$

where $w[n]$ is i.i.d. complex Gaussian noise. When the system performs cyclic prefix insertion and removal, and IFFT and FFT operations, the model in Eq. (1) can be represented in the frequency domain as

$$Y[k] = H[k]X[k] + W[k], \quad k \in [0, N-1] \quad (2)$$

In practice, the actual length of the channel L_h is unknown. The receiver uses an estimated channel length L , which is either determined before deployment or adaptively estimated.

The signal \mathbf{X} consists of all N subcarriers, with pilots placed in subcarriers $k \in \mathcal{K}_p$ and data placed in subcarriers $k \in \mathcal{K}_d$. The remaining N_{null} subcarriers are split between the two band edges and indexed as $k \in \mathcal{K}_{\text{null}}$ such that the frequency domain signal $\mathbf{X} = [X[0] \cdots X[N-1]]^T$ has elements

$$X[k] = \begin{cases} 0 & k \in \mathcal{K}_{\text{null}} \\ P_k & k \in \mathcal{K}_p \\ S_k & k \in \mathcal{K}_d \end{cases}, \quad (3)$$

where P_k is the pilot in the k^{th} subcarrier and S_k is the data in the k^{th} subcarrier.

For convenience, we define the submatrices \mathbf{Q}_p and \mathbf{Q}_d of the N by N discrete Fourier transform matrix with elements defined as $[\mathbf{Q}_p]_{kl} = \frac{1}{\sqrt{N}} e^{-j\frac{2\pi kl}{N}}$, for $k \in \mathcal{K}_p$ and $l \in [0, L-1]$ and $[\mathbf{Q}_d]_{kl} = \frac{1}{\sqrt{N}} e^{-j\frac{2\pi kl}{N}}$, for $k \in \mathcal{K}_d$ and $l \in [0, L-1]$. We also use the notation $\mathbf{Y}[\mathcal{K}_p]$ to denote the vector containing the elements $Y[k]$, $k \in \mathcal{K}_p$, and $|\mathbf{Y}|^\kappa[\mathcal{K}_p]$ to represent the vector containing the magnitude of each of the elements in $\mathbf{Y}[\mathcal{K}_p]$ raised to the κ^{th} power.

Given the model in Eq. (2) and Eq. (3), and assuming the real channel length L is known, true wireless channel for the data subcarriers $\mathbf{H}[\mathcal{K}_d]$ can be estimated using the method of least-squares [14, p. 529]. If statistics of the channel are also known, techniques such as Bayesian channel estimation [14, p. 533] could be used to provide a more accurate estimate. In this paper, we only consider the least-squares channel estimate, which is given as [14, p. 529]

$$\hat{\mathbf{H}}[\mathcal{K}_d] = \mathbf{Q}_d \left(\mathbf{Q}_p^H \mathbf{D}_{\mathbf{X}[\mathcal{K}_p]} \mathbf{D}_{\mathbf{X}[\mathcal{K}_p]} \mathbf{Q}_p \right)^{-1} \mathbf{Q}_p^H \mathbf{D}_{\mathbf{X}[\mathcal{K}_p]} \mathbf{Y}[\mathcal{K}_p], \quad (4)$$

where $\mathbf{D}_{\mathbf{X}[\mathcal{K}_p]}$ denotes the diagonal matrix containing the elements $X[k]$, $k \in \mathcal{K}_p$ in its diagonal.

The covariance matrix of this channel estimate can be calculated as

$$\mathbf{C}_{\hat{\mathbf{H}}[\mathcal{K}_d]} = \mathbf{Q}_d \left(\mathbf{Q}_p^H \mathbf{D}_{|\mathbf{X}|^2[\mathcal{K}_p]} \mathbf{Q}_p \right)^{-1} \mathbf{Q}_p^H \mathbf{D}_{\mathbf{X}[\mathcal{K}_p]} \mathbf{C}_w \mathbf{D}_{\mathbf{X}[\mathcal{K}_p]} \mathbf{Q}_p \left(\mathbf{Q}_p^H \mathbf{D}_{|\mathbf{X}|^2[\mathcal{K}_p]} \mathbf{Q}_p \right)^{-H} \mathbf{Q}_d^H, \quad (5)$$

where \mathbf{C}_w is the covariance matrix of the noise present in the pilot positions at the receiver. We consider the pilot design problem with the objective of minimizing the MSE of the channel estimate $\epsilon = \frac{1}{N_d} \text{tr}(\mathbf{C}_{\hat{\mathbf{H}}[\mathcal{K}_d]})$ (where $\text{tr}(\mathbf{A})$ denotes the trace of \mathbf{A}) by optimizing the indices of pilot subcarriers \mathcal{K}_p and allocated pilot power $|X_k|^2$, $k \in \mathcal{K}_p$ to these subcarriers.

III. PILOT POWER OPTIMIZATION

We first consider the problem of determining how power should be allocated among an arbitrary set of pilots. Current methods have adopted convex optimization [4]–[8] to numerically calculate the power profile that minimizes the norm of either the channel estimate error or data estimate error. Instead, we consider the case where the number of channel taps is equal to the number of pilots (i.e., $L = N_p$), and derive an analytical solution for the optimal power allocation which minimizes the channel estimate MSE.

A. Deriving the optimal power profile

Since the noise term $w[k]$ is i.i.d., $\mathbf{C}_w = \sigma_w^2 \mathbf{I}$, we can rewrite Eq. (5) as

$$\mathbf{C}_{\hat{\mathbf{H}}[\mathcal{K}_d]} = \sigma_w^2 \mathbf{Q}_d \left(\mathbf{Q}_p^H \mathbf{D}_{|\mathbf{X}|^2[\mathcal{K}_p]} \mathbf{Q}_p \right)^{-1} \mathbf{Q}_d^H. \quad (6)$$

If the true channel length L is unknown, the worst case is that the number of taps in the channel is equal to the number of pilots. Designing for the worst case, we have $L = N_p$ and \mathbf{Q}_p is square. Thus Eq. (6) can be simplified as

$$\mathbf{C}_{\hat{\mathbf{H}}[\mathcal{K}_d]} = \sigma_w^2 \mathbf{Q}_d \mathbf{Q}_p^{-1} \mathbf{D}_{|\mathbf{X}|^2[\mathcal{K}_p]}^{-1} \left(\mathbf{Q}_d \mathbf{Q}_p^{-1} \right)^H.$$

For convenience we define the matrix $\mathbf{\Gamma} = \mathbf{Q}_d \mathbf{Q}_p^{-1}$, so the channel estimate MSE is given by

$$\begin{aligned} \epsilon &= \frac{\sigma_w^2}{N_d} \text{tr} \left(\mathbf{\Gamma} \mathbf{D}_{|\mathbf{X}|^2[\mathcal{K}_p]}^{-1} \mathbf{\Gamma}^H \right) \\ &= \frac{\sigma_w^2}{N_d} |\mathbf{X}^T|^{-2} [\mathcal{K}_p] \text{diag}(\mathbf{\Gamma}^H \mathbf{\Gamma}), \end{aligned} \quad (7)$$

which is the vector product of the row vector $|\mathbf{X}|^2[\mathcal{K}_p]$ and the column vector $\text{diag}(\mathbf{\Gamma}^H \mathbf{\Gamma})$ containing the diagonal elements of $\mathbf{\Gamma}^H \mathbf{\Gamma}$. In the absence of null subcarriers, the optimal pilot design achieves a channel estimate MSE of $\epsilon_{\text{opt}} = \frac{\sigma_w^2}{|\mathbf{X}|^2}$ where $|\mathbf{X}|^2$ is the average power in the pilots. In the presence of null subcarriers we can define a lower bound for the channel MSE as $\frac{L}{N_p} \frac{N - N_{\text{null}}}{N} \frac{\sigma_w^2}{|\mathbf{X}|^2}$. We define the normalized mean-squared error (NMSE) as the ratio between the MSE and the MSE of the optimal design without null subcarriers MSE

$$\text{NMSE} = \epsilon / \epsilon_{\text{opt}}. \quad (8)$$

Since we assume $L = N_p$, this NMSE then can then range from $\frac{N - N_{\text{null}}}{N}$ to ∞ .

Eq. (7) can be rewritten as

$$\epsilon = \frac{\sigma_w^2}{N_d} \sum_{n=0}^{N_d-1} \sum_{i=0}^{N_p-1} \frac{|\Gamma_{ni}|^2}{|X[k_i]|^2}, \quad (9)$$

where Γ_{ni} is the element in the n^{th} row and i^{th} column of $\mathbf{\Gamma}$ and k_i is the i^{th} element in \mathcal{K}_p . We can then define the MSE of the channel estimate in each data subcarrier n as

$$\epsilon_n = \sigma_w^2 \sum_{i=0}^{N_p-1} \frac{|\Gamma_{ni}|^2}{|X[k_i]|^2}, \quad (10)$$

and the corresponding subcarrier NMSE as the ratio

$$\text{NMSE}_n = \epsilon_n / \epsilon_{\text{opt}}. \quad (11)$$

The optimum power profile is found by minimizing Eq. (9) with respect to $|X[k_i]|^2$ with the constraint that $\sum_{i=0}^{N_p-1} |X[k_i]|^2 = 1$:

$$|X_{\text{opt}_i}|^2 = \arg \min_{|X[k_i]|^2, \lambda} \frac{\sigma_w^2}{N_d} \sum_{n=0}^{N_d-1} \sum_{i=0}^{N_p-1} \frac{|\Gamma_{ni}|^2}{|X[k_i]|^2}. \quad (12)$$

By solving Eq. (12) with the total power constraint, we have

$$|X_{\text{opt}_i}|^2 = \frac{\sqrt{\sum_{n=0}^{N_d-1} |\Gamma_{ni}|^2}}{\sum_{m=0}^{N_p-1} \sqrt{\sum_{n=0}^{N_d-1} |\Gamma_{nm}|^2}}. \quad (13)$$

Using the power profile in Eq. (13), we find the resulting MSE as

$$\epsilon_{\text{opt}} = \frac{\sigma_w^2}{N_d} \left(\sum_{i=0}^{N_p-1} \sqrt{\sum_{n=0}^{N_d-1} |\Gamma_{ni}|^2} \right)^2. \quad (14)$$

B. Analytical Solution for Γ

In the previous section, Γ was defined as $\Gamma = \mathbf{Q}_d \mathbf{Q}_p^{-1}$. The calculation of Γ using this definition relies on calculating the inverse of the matrix \mathbf{Q}_p . In systems with large number of subcarriers, however, \mathbf{Q}_p is nearly singular and thus suffers from inaccuracies due to the lack of sufficient numerical precision. In this section we derive an analytical expression for Γ which does not suffer from these deficiencies.

We note that both \mathbf{Q}_p and \mathbf{Q}_d are Vandermonde matrices. From [15], the inverse of \mathbf{Q}_p , \mathbf{Q}_p^{-1} , is the Lagrange basis of \mathbf{Q}_p . The m^{th} column of the Lagrange basis of \mathbf{Q}_p are the coefficients of x in the interpolation polynomial (shown here in Lagrange form): $\ell_m(x) = \prod_{n=0, n \neq m}^{N_p-1} \frac{x - x_n}{x_m - x_n}$, where $x_m = e^{-j \frac{2\pi k_{pm}}{N}}$, and k_{pm} is the m^{th} element in \mathcal{K}_p .

Since \mathbf{Q}_d is also Vandermonde and is multiplied by the coefficients of the interpolation polynomial of \mathbf{Q}_p , the elements Γ_{ni} of Γ are simply equal to $\ell_i(x)$ evaluated at $x = e^{-j \frac{2\pi k_{dn}}{N}}$, where k_{dn} is the n^{th} element in \mathcal{K}_d :

$$\Gamma_{ni} = \prod_{m=0, m \neq i}^{N_p-1} \frac{e^{-j \frac{2\pi k_{dn}}{N}} - e^{-j \frac{2\pi k_{pm}}{N}}}{e^{-j \frac{2\pi k_{pi}}{N}} - e^{-j \frac{2\pi k_{pm}}{N}}}. \quad (15)$$

We then split Eq. (15) so that

$$\Gamma_{ni} = \gamma_{dn} \gamma_{pi}^{-1} \left(e^{-j \frac{2\pi k_{dn}}{N}} - e^{-j \frac{2\pi k_{pi}}{N}} \right)^{-1}, \quad (16)$$

$$\gamma_{dn} = \prod_{m=0}^{N_p-1} e^{-j \frac{2\pi k_{dn}}{N}} - e^{-j \frac{2\pi k_{pm}}{N}}$$

$$\gamma_{pi} = \prod_{m=0, m \neq i}^{N_p-1} e^{-j \frac{2\pi k_{pi}}{N}} - e^{-j \frac{2\pi k_{pm}}{N}}$$

Splitting the equation this way reduces the complexity since the entries in the vectors γ_d and γ_p can be calculated once and then used to generate all the entries of Γ .

This analytical solution for the optimal pilot profile requires significantly less computation than the iterative gradient-descent convex optimizations which have been presented in the literature, and produces the globally optimal power profile

solution. In practice, we have found that the pilot power profiles produced by our analytical solution avoid numerical instabilities encountered by some existing methods [4]–[8] relying on convex optimizations. Since our solution avoids those problems, it is able to obtain pilot designs that result in lower channel estimate error than conventional methods.

IV. PILOT POSITION OPTIMIZATION

While the 3rd order parameterized pilot design presented in [4] provides a design nearly optimal for simple systems such as the 256 subcarrier system with 8 pilots and 56 null subcarriers originally analyzed, designs for systems with larger numbers of subcarriers, channel taps and null subcarriers experience a substantial degradation in performance since this design puts too few pilots in the center of the band. We present a framework for higher order parameterizations which offers improved performance.

Similar to the 3rd order parameterization [4], we parameterize the pilot sequence with a polynomial function $p(x)$, which maps the pilot indices to the subcarrier indices for each pilot. The input of the function is the pilot index, consisting of integers from 0 to $N_p - 1$. The output of this function is the pilot position, consisting of integers from 0 to $N - 1$. In contrast to [4], we decompose the function into three parts such that $p(x) = f(g(h(x)))$. Define $f(x) = \lfloor \alpha x + N/2 \rfloor$ and $h(x) = x/\eta - 1$, where $\alpha = \frac{N_d + N_p - 1}{2}$, $\eta = \frac{N_p - 1}{2}$, and $\lfloor \cdot \rfloor$ denotes the rounding operation. Decomposing $p(x)$ this way simplifies the derivation below by shifting the input and output of $g(x)$ so that it is centered on the intersection of the x and y axes and ranges from $g(-1) = -1$ to $g(1) = 1$ regardless of the system being designed. We parameterize the remaining function $g(x)$ as the order P polynomial $g(x) = \sum_{n=0}^P a_n x^n$, where a_n are the design parameters. When $P = 3$, this generic parameterization will be equivalent to the 3rd order design in [4].

Our goal is to find the coefficients $\{a_n\}_{n=0}^P$ that minimize the channel estimate MSE. This will be accomplished using a grid search over the $P + 1$ dimensional set \mathcal{A}_P . For general P order polynomials, $\mathcal{A}_P = \{a_n | a_n \in \mathbb{R}, n \in \{0, \dots, P\}\}$, which is a very large search space. Fortunately, in the context of our problem, we can decrease the search space $\tilde{\mathcal{A}}_P \subset \mathcal{A}_P$ to ease the grid search complexity by applying the following three constraints:

- C1 The resulting pilot profile should be symmetric, i.e., $g(x) = -g(-x)$, or that $g(x)$ is an odd function.
- C2 The function $g(x)$ should only map pilots onto subcarriers that are in the band. Thus, we impose that $g(1) = 1$ and $g(-1) = -1$. Due to the symmetry caused by the first constraint these two expressions are equivalent.
- C3 The function should return the pilots in order and no pilot should be duplicated. This means that $g(x)$ must be a monotonically increasing function within the band. Hence, $g'(x) > 0$ for $-1 \leq x \leq 1$.

We can apply these constraints to the polynomial $g(x)$ as follows: Based on constraint C1, we can drop the even order terms from $g(x)$. After applying this constraint, we have $g(x) = \sum_{m=0}^D a_{2m+1} x^{2m+1}$, where $D = \lfloor (P - 1)/2 \rfloor$. Using constraint C2, we can solve for a_1 as $a_1 = 1 -$

$\sum_{m=1}^D a_{2m+1} x^{2m+1}$. Constraint C3 can be used to bound the additional parameters. Although there is no general analytic bound which guarantees constraint C3 is satisfied, we can define the set

$$\begin{aligned} \hat{\mathcal{A}}_P &= \{a_{2k+1} | a_{2k+1} \in \mathbb{R}, k \in \{0, \dots, D\}, \\ 1 - \sum_{m=1}^D a_{2m+1} &\geq 0, 1 + \sum_{m=1}^D 2ma_{2m+1} \geq 0\} \end{aligned} \quad (17)$$

as a bound on $\tilde{\mathcal{A}}_P$, such that $\hat{\mathcal{A}}_P \supseteq \tilde{\mathcal{A}}_P$.

The optimal pilot profile can then be found by performing a grid search over the design parameters $a_3 \dots a_{2D+1}$ and calculating the error of the pilot positions at each point using either Eq. (14) or some other optimization such as those proposed in [4]–[8]. The optimal pilot design is taken as the design from the grid search with the minimum error. The grid search does add a significant amount of computational cost to the design, however it can be computed offline when the design is being standardized¹.

For the 3rd order design, the bounds in Eq. (17) are tight, so that

$$\hat{\mathcal{A}}_3 = \tilde{\mathcal{A}}_3 = \{a_n | -0.5 \leq a_3 \leq 1, a_1 = 1 - a_3, n \in \{1, 3\}\}.$$

The 5th order design is found similarly. From the generic design, we can apply constraint C3 to find the tight bound. We also apply the constraint that $a_5 \leq 0$. This constrains the shape of $g(x)$ so that pilots will be more dense on both the edges and the center, which is what we expect from the optimum design. The resulting search area is contained in the region

$$\begin{aligned} \tilde{\mathcal{A}}_5 &= \{a_n | a_1 = 1 - a_3 - a_5, -0.5 \leq a_3 \leq 2.5, \\ &\quad \mathcal{C}_5, n \in \{1, 3, 5\}\}, \end{aligned}$$

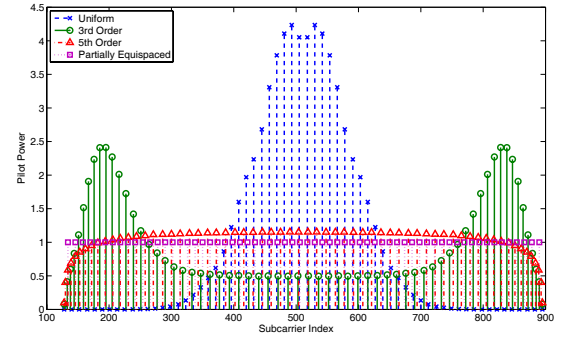
where \mathcal{C}_5 is defined as

$$\mathcal{C}_5 = \left\{ a_5 \left| \begin{array}{ll} -0.25 - 0.5a_3 \leq a_5 \leq 0, & -0.5 \leq a_3 \leq 1 \\ -0.25 - 0.5a_3 \leq a_5 \leq 1 - a_3, & 1 \leq a_3 \leq 2.5 \end{array} \right. \right\} \quad (18)$$

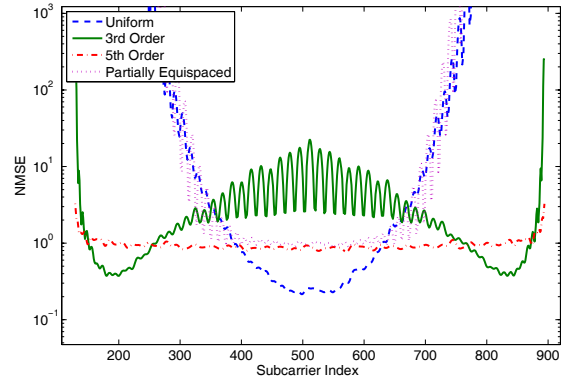
V. NUMERICAL RESULTS

In this section we compare the NMSE (defined in (8)) and BER of the 5th order parameterized design to existing designs. We compare with the partially equispaced design [12], and the iterative reduction design previously proposed by Ohno et al. [8]. The power profile optimization described in Section III was used to calculate the pilot power profile for both the 3rd and 5th order parameterizations as well as a partially equispaced design. We will refer to this partially equispaced design with the power profile optimization as ‘uniform’. We employed a grid search across a_3 for the 3rd order scheme in [4] and a_5 and a_3 for the 5th order to find the optimal pilots.

¹Higher order designs such as a 7th order design are simple extensions of this framework. Such higher order designs will require a significant amount of computation and may require the computation to be distributed over a large computer cluster.



(a) Pilot Design



(b) Subcarrier Channel Estimation NMSE

Fig. 1. Pilot Design and subcarrier NMSE for system with $N = 1024$, $N_p = 64$, $N_{\text{null}} = 256$.

Subcarrier Channel Estimate MSE: We first examined the pilot allocation and subcarrier channel estimate NMSE (defined in (11)) in a system with $N = 1024$ subcarriers with $N_{\text{null}} = 268$ null subcarriers and $N_p = 64$ pilots. The pilot designs are shown in Figure 1(a), and the resulting channel estimate NMSEs are compared in Figure 1(b). The uniform placement has extremely high NMSE on the edges and low NMSE in the center, suggesting that pilots should be shifted away from the center and towards the edges. The 3rd order design, in contrast, has a higher NMSE both in the middle and on the band edges. This suggests that the 3rd order parameterization is not flexible enough to provide a high pilot density on the band edges without reducing pilot density in the center excessively. In contrast, the 5th order parameterized design results in a much lower, flatter NMSE, suggesting that this parameterization better approximates the optimal pilot distribution.

Increasing N , N_p and N_{null} proportionally: Next we examined the NMSE when the number of null and pilot subcarriers were increased proportionally to the number of subcarriers such that $N_{\text{null}} = N/4$ and $N_p = N/8$. This sort of scaling is common in standards such as Digital Video Broadcasting[16]. We use this simulation to demonstrate how the 5th order design scales with increasing complexity. By increasing the number of nulls and pilots proportionally, we can compare systems where the pilot density distribution should be similar. The channel estimate NMSE was determined both theoretically from Eq. (14) and using Monte Carlo

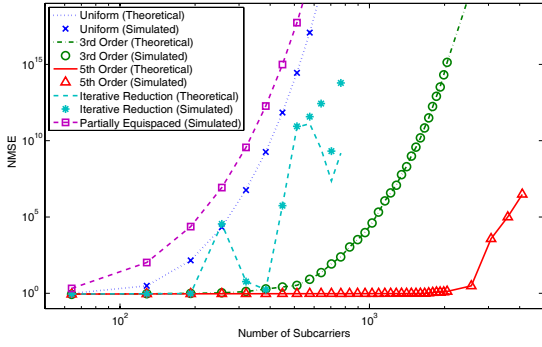


Fig. 2. Channel NMSE vs Number of Subcarriers (proportional)

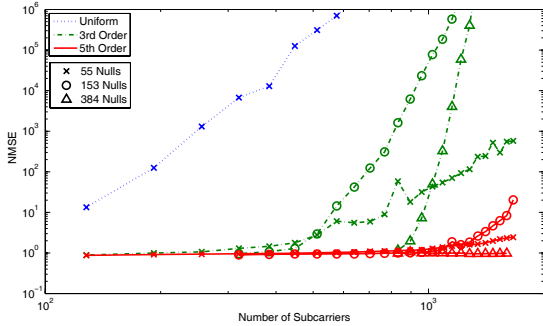


Fig. 3. Channel NMSE vs Number of Subcarriers (fixed Nulls)

simulation. In Figure 2, the theoretical NMSE calculated using Eq. (14) closely matches the simulated results for most of the plots, validating the theoretical results. Additionally, the plot shows that the 5th order design scales much better, retaining near optimal performance for systems with significantly more subcarriers than the other methods compared.

Increasing N , with N_{null} fixed: We then compared the NMSE when the number of nulls were fixed and the number of pilot subcarriers were increased proportionally to the number of subcarriers such that $N_p = N/8$. Increasing the number of subcarriers this way is analogous to adding subcarriers by increasing the bandwidth of the system (as opposed to adding subcarriers by decreasing the bandwidth of each subcarrier). From Figure 3, it is apparent that the 5th order design offers a lower NMSE than existing methods.

NMSE when $L < N_p$: The pilot power optimization in Section III assumed $L = N_p$. We compare the NMSE of designs using our analytical power optimization in Section III with designs using an approximate power optimization based on convex optimization [4], [5]. The results for a 1024 subcarrier system are shown in Figure 4. The plots denoted by $L \neq N_p$ are the designs using the convex optimization. From the figure, the analytical solution offers similar MSE as the convex optimization for a wide range of L/N_p , despite only being optimal for $L = N_p$. Further, the MSE of the convex optimization fluctuates significantly due to the effects of numerical instability. These figures also show that, while for systems where $L \ll N_p$ the partially equispaced design [12] is preferable, larger systems with longer channels benefit greatly from our proposed design.

Bit Error Rate: We examined the BER in Figure 5. The channel was modeled as an FIR filter with complex Gaussian

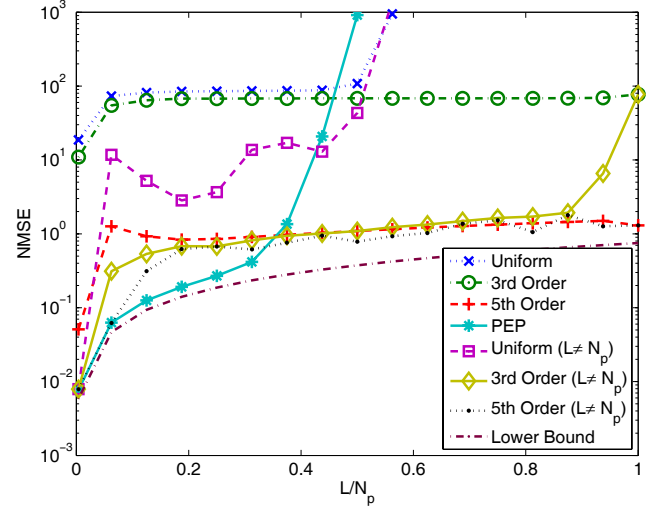
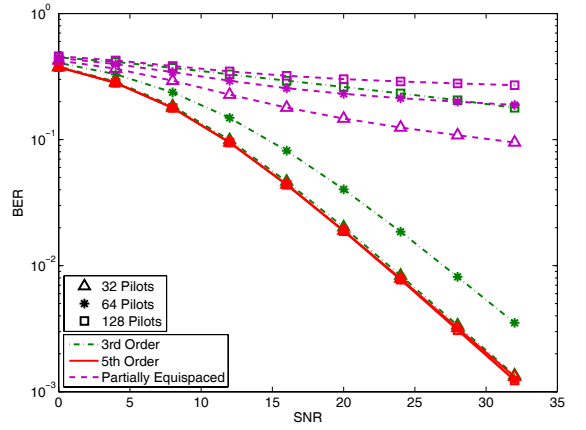
Fig. 4. Channel NMSE with $L \leq N_p$ for a system with 1024 subcarriers

Fig. 5. Data BER vs SNR (1024 Subcarriers)

random taps of constant power such that the total power in the channel was 1. This figure shows the BER for a system with 1024 subcarriers as a function of signal-to-noise ratio (SNR). The larger channel estimate MSE from the Uniform and 3rd order designs severely degrades the data BER in this system, even in high SNR. Only the 32-pilot 3rd order design approaches the 5th order design BER. In contrast the 5th order design we proposed has a significantly lower BER due to the higher accuracy of its channel estimates.

VI. CONCLUSION

We have presented a new pilot design technique for channel estimation in OFDM systems employing null subcarriers. This technique combines a 5th order parameterization of pilot position with an analytical solution for pilot power. We showed that this new technique is able to design pilots that offers a substantial improvement over those existing methods in systems employing large numbers of subcarriers.²

²The views and conclusions contained in this document are those of the authors and should not be interpreted as representing the official policies, either expressed or implied, of the Army Research Laboratory or the U. S. Government.

REFERENCES

- [1] IEEE Standard for Local and Metropolitan Area Networks Part 16: Air Interface for Broadband Wireless Access Systems, IEEE Std. 802.16-2009 (Revision of 802.16-2004), 2009.
- [2] Z. Wang and G. Giannakis, "Wireless multicarrier communications," *IEEE Signal Process. Mag.*, vol. 17, no. 3, pp. 29–48, May 2000.
- [3] J. Cavers, "An analysis of pilot symbol assisted modulation for Rayleigh fading channels," *IEEE Trans. Veh. Technol.*, vol. 40, no. 4, pp. 686–693, Nov 1991.
- [4] R. J. Baxley, J. E. Kleider, and G. T. Zhou, "Pilot design for IEEE 802.16 OFDM and OFDMA," in *Proc. IEEE ICASSP*, vol. 2, Apr. 2007, pp. 321–324.
- [5] —, "Pilot design for OFDM with null edge subcarriers," *IEEE Trans. Wireless Commun.*, vol. 8, no. 1, pp. 396–405, Jan. 2009.
- [6] S. Ohno, "Preamble and pilot symbol design for channel estimation in OFDM," in *Proc. IEEE ICASSP*, vol. 3, 2007.
- [7] S. Ohno, S. Hosokawa, and K. A. D. Teo, "Pilot power optimization for channel estimation in OFDM systems," in *Proc. APCC*, 2008, pp. 1–5.
- [8] S. Ohno, E. Manasseh, and M. Nakamoto, "Pilot symbol design for channel estimation in OFDM with null subcarriers," in *Proc. Asia-Pacific Signal and Information Processing*, Oct. 2009, pp. 696–699.
- [9] R. Negi and J. Cioffi, "Pilot tone selection for channel estimation in a mobile OFDM system," *IEEE Trans. Consum. Electron.*, vol. 44, no. 3, pp. 1122–1128, 1998.
- [10] M. Morelli and U. Mengali, "A comparison of pilot-aided channel estimation methods for OFDM systems," *IEEE Trans. Signal Process.*, vol. 49, no. 12, pp. 3065–3073, Dec. 2001.
- [11] D. Hu, L. Yang, Y. Shi, and L. He, "Optimal pilot sequence design for channel estimation in MIMO OFDM systems," *IEEE Commun. Lett.*, vol. 10, no. 1, pp. 1–3, 2006.
- [12] S. Song and A. C. Singer, "Pilot-aided OFDM channel estimation in the presence of the guard band," *IEEE Trans. Commun.*, vol. 55, no. 8, pp. 1459–1465, 2007.
- [13] Q. Huang, M. Ghogho, and S. Freear, "Pilot design for MIMO OFDM systems with virtual carriers," *IEEE Trans. Signal Process.*, vol. 57, pp. 2024–2029, May 2009.
- [14] S. M. Kay, *Fundamentals of Statistical Signal Processing: Estimation Theory*, 1st edition. Prentice Hall, 1993.
- [15] M. E. A. El-Mikkawy, "Explicit inverse of a generalized vandermonde matrix," *Appl. Mathematics Computation*, vol. 146, no. 2-3, pp. 643–651, 2003.
- [16] Frame structure, channel coding and modulation for a second generation digital terrestrial television broadcasting system (DVB-T2), ETSI Std. EN 302 755, Rev. 1.1.1, Aug. 2009.